

Photoluminescence and electro-optic properties of small (25–35 nm diameter) quantum boxes

L. Davis, K. K. Ko, W.-Q. Li, H. C. Sun, Y. Lam, T. Brock, S. W. Pang,
and P. K. Bhattacharya

*Solid State Electronics Laboratory, Department of Electrical Engineering and Computer Science,
The University of Michigan, Ann Arbor, Michigan 48109-2122*

M. J. Rooks

National Nanofabrication Facility, Cornell University, Ithaca, New York 14853

(Received 14 December 1992; accepted for publication 3 April 1993)

The luminescence and electro-optic properties of buried 25–35 nm quantum boxes have been measured. The quantum boxes were defined by a combination of molecular beam epitaxial growth and regrowth, electron beam lithography, and dry etching. The photoluminescence from 35 nm boxes shows a blue shift of ~ 15 meV compared to the bulk luminescence and an enhancement, taking into account the fill factor. An enhanced effective linear electro-optic coefficient, r_p , is observed for the quantum boxes.

Research on lower-dimensional quantum confined structures such as quantum boxes and quantum wires has been fueled by the implications in physics and the quest for structures with enhanced oscillator strengths and resulting luminescence intensity.^{1,2} In addition, such nanostructures are expected to exhibit enhanced optical nonlinearities and enhanced electro-optic properties.^{3,4} In a device such as a junction laser, the insertion of quantum boxes and wires in the active recombination volume is expected to lower the threshold current through the modification of the density-of-states function and differential gain.^{5,6}

Since such structures usually have a large surface-to-volume ratio, their luminescent properties are intimately related to the fabrication technique. It has been shown and suggested that both extrinsic effects such as surface and interfacial disorder and intrinsic phenomena such as phonon scattering rates can wipe out most of the expected advantages and degrade the luminescent properties.^{7–9} The realization of quantum boxes and wires has proceeded along several lines, including growth on vicinal surfaces,¹⁰ selective and nonselective epitaxy on patterned substrates,^{11,12} strain-induced lateral confinement,¹³ and nanolithography using electron- or ion-beam techniques.^{14–16} The last technique is usually accompanied by epitaxial overgrowth to create an enclosed structure.

In the present study, we have used the last technique, which is conceptually the simplest, to realize very small (25–35 nm) quantum boxes. The luminescence from these structures shows an enhancement in intensity compared to the quantum wells, when the fill factor is taken into account. More importantly, we have made waveguides with an array of such boxes and have measured the electro-optic coefficients of these modulator structures.

All the samples used were grown by molecular beam epitaxy (MBE) on (100) Si-doped GaAs substrate. They consisted of a 300 nm GaAs layer ($n=5 \times 10^{17}$ cm⁻³), a 200 nm graded GaAs to Al_{0.55}Ga_{0.45}As layer ($n=5 \times 10^{17}$ cm⁻³), a 600 nm Al_{0.55}Ga_{0.45}As layer ($n=5 \times 10^{17}$ cm⁻³), a 200 nm graded Al_{0.55}Ga_{0.45}As to GaAs layer (undoped), a 20 nm undoped GaAs layer, 4 undoped quantum wells

made up of 7 nm GaAs and 8 nm In_xGa_{1-x}As ($x=0.1$ and 0.15), and a 20 nm undoped GaAs cap layer. Electron beam lithography was used for direct writing of the quantum boxes on a bilayer of polymethylmethacrylate (PMMA). A subsequent liftoff process using 20 nm Ni formed the mask for dry etching. The quantum box array for photoluminescence (PL) measurements covered a 100×80 μm^2 area, and consisted of boxes which were 35 nm in diameter with 200 nm pitch. The fill factor for this array is $\sim 2.5\%$. Arrays with boxes that were 25 nm in diameter and 100 nm pitch were also fabricated.

Free-standing quantum boxes were then defined by dry etching using an electron cyclotron resonance (ECR) source and a rf-powered electrode.¹⁷ The GaAs capping layer and the 4 quantum wells were etched using either a Cl₂/N₂ or Cl₂/Ar mixture with etch rates ranging from 23 to 38 nm/min. The etching was controlled to within 20 nm below the last InGaAs well. This is important to avoid incomplete sidewall coverage and the formation of aluminum oxide on the Al_{0.55}Ga_{0.45}As surface before MBE regrowth. Figure 1 shows the quantum boxes after direct electron beam writing, 20 nm Ni liftoff, and dry etching using the ECR source. Buried quantum boxes were real-

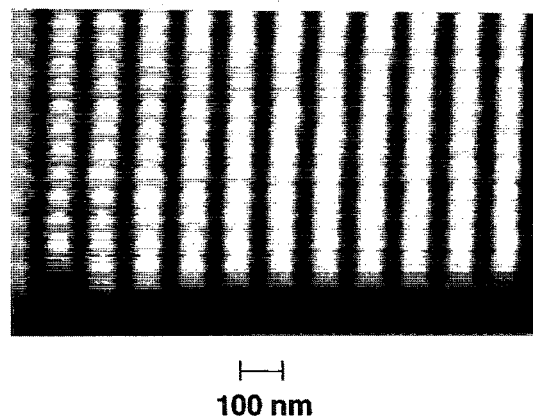


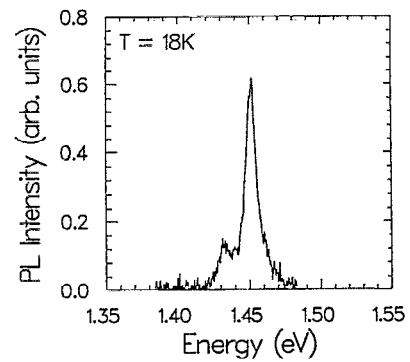
FIG. 1. SEM micrograph of the quantum boxes after direct electron beam writing, 20 nm Ni liftoff, and dry etching using an ECR source.

ized by MBE epitaxial regrowth. Before loading the samples into the MBE chamber, a warm solvent clean (trichloromethane, acetone, and isopropyl alcohol), a 5 min O_2 plasma ashing at 100 W, and a native oxide etch in $HCl:H_2O=1:1$ were performed. A 10 min desorption of the surface oxide was done at 600 °C. The regrown structures consisted of a 100 nm undoped GaAs layer, a 200 nm graded GaAs to $Al_{0.55}Ga_{0.45}As$ layer (undoped), a 500 nm $Al_{0.55}Ga_{0.45}As$ layer ($p=5 \times 10^{17} \text{ cm}^{-3}$), a 100 nm $Al_{0.55}Ga_{0.45}As$ to GaAs layer ($p=5 \times 10^{17} \text{ cm}^{-3}$), and a 20 nm GaAs layer ($p=1 \times 10^{18} \text{ cm}^{-3}$). We have extensively studied regrowth using MBE technology,¹⁸ and from control regrowth experiments with step heights of various sizes we believe that the dots in this experiment are perfectly embedded in the 100 nm undoped GaAs layer.

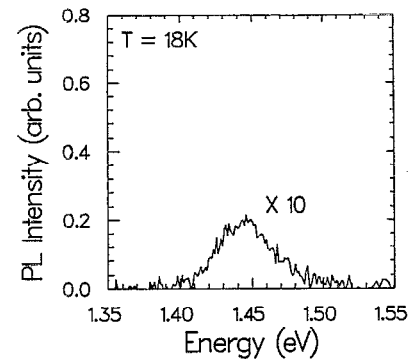
In order to carry out electro-optic measurements on the samples, single-mode waveguides, with the buried box array as the guiding region, were fabricated by standard lithography and dry etching. Top p -type and backside n -type ohmic contacts were formed by electron-beam evaporation. All the waveguides are 3 μm wide and 900 μm long, formed by cleaving along the (110) plane.

Low-temperature PL measurements were made using the 532 nm output of a frequency-doubled Nd:YAG laser as an excitation source and a 0.5 m scanning spectrometer. The PL samples were similar to those used for the waveguiding measurement, with the notable difference being the replacement of the GaAs etch stop layer with a 15 nm InGaAs etch stop layer for reference emission in the PL spectra. Figure 2(a) shows the PL spectra of the as-grown $In_{0.10}Ga_{0.90}As$ quantum wells. A strong bound exciton peak is observed at 1.451 eV accompanied by a weaker transition at 1.432 eV. We believe the latter results from recombination in the 15 nm $In_{0.10}Ga_{0.90}As$ layer below the quantum wells. Therefore, the transition energy includes some quantization effects. The PL spectrum of a 35 nm quantum box after dry etching and regrowth is shown in Fig. 2(b). The intensity of the luminescence is lowered by a factor of 30 compared to the quantum well luminescence, but when the fill factor is taken into account, there is actually a slight enhancement in the intensity. The peak is blue shifted from the weak $In_{0.10}Ga_{0.90}As$ luminescence of Fig. 2(a) by ~ 15 meV and it can be shown that it is blue-shifted from the bulk $In_{0.10}Ga_{0.90}As$ luminescence energy by a little more. In our experiment, the energy of the excitation source is approximately 880 meV above the observed PL transition energy in the box. In 0D or quasi-0D structures, due to the drastic reduction of phonon scattering rates by the so-called phonon bottleneck problem,⁹ orders-of-magnitude reduction in the quantum efficiency of dots of size less than several hundred angstroms is predicted.^{8,9} The fact that we observed luminescence, even with 35 nm dots, suggests that interface scattering or some other similar scattering phenomena helps the excited carriers to relax to the levels from which they recombine.

It has been predicted² and demonstrated¹⁵ that one- and zero-dimensional quantum confined structures will demonstrate enhanced electro-optic properties compared



(a)



(b)

FIG. 2. The PL spectra of (a) the as-grown $In_{0.10}Ga_{0.90}As$ quantum wells, and (b) 35 nm quantum boxes after dry etching and regrowth.

to bulk and two-dimensional structures. We have therefore made measurements of the electro-optic coefficient and voltage-induced phase shift in waveguide structures whose guiding regions are either quantum wells or quantum boxes with regrown cladding layers, such as that shown in Fig. 3. We have examined two different waveguiding structures: in

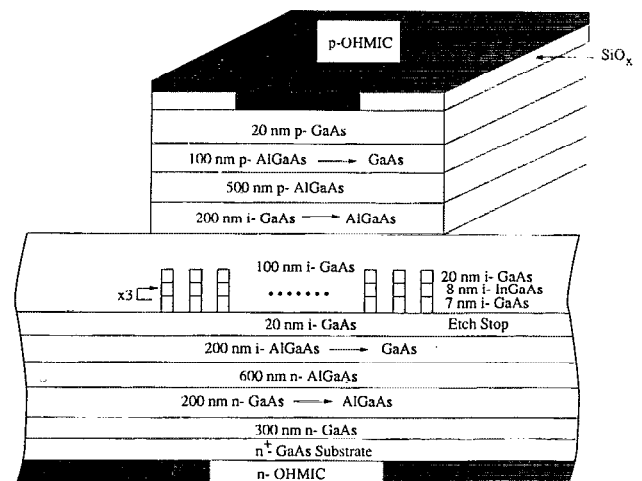


FIG. 3. The waveguiding structure, showing the location of the quantum boxes.

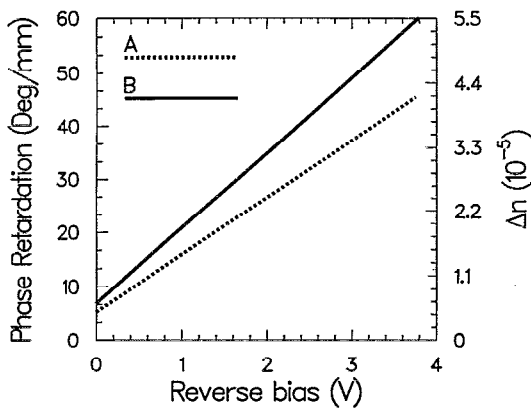


FIG. 4. Best-fit lines to the relative phase retardation as a function of reverse bias.

sample A, only 300 μm of the 900 μm waveguide has quantum boxes in the guiding region; and in sample B, the entire 900 μm waveguide has quantum boxes in the guiding region. The measurement was carried out by end-fire launching a linearly polarized laser beam into the waveguide with a single mode polarization preserving fiber. The excitation source was a 1.15 μm HeNe laser. The light is launched in order to excite both ordinary and extraordinary modes in the waveguide. Phase retardation of the transmitted light was then measured using a Ge detector and the usual polarizer-analyzer arrangement. The measured phase retardation was observed to vary roughly linearly with the reverse bias applied (perpendicularly) to the waveguide. The linear electro-optic coefficient describing this relation was then calculated using the slope of the best-fit straight line relating the experimental phase retardation changes to the applied reverse bias (Fig. 4). The electro-optic coefficients were extracted from the phase retardation data assuming the standard relation for (001)-oriented zincblende crystals,¹⁹ $\Delta\Phi = (\pi L/\lambda)n^3r_lE\zeta$, where $\Delta\Phi$ is the phase shift, L is the length, r_l is the linear electro-optic coefficient, E is the electric field applied perpendicular to the waveguide, and ζ is the overlap integral. In our calculation, an overlap integral of 6% between the optical mode and the applied electric field was assumed. The effective linear electro-optic coefficients extracted for the two different waveguides with $\text{In}_{0.15}\text{Ga}_{0.85}\text{As}$ active regions is 5.9×10^{-12} m/V for sample A, and 6.3×10^{-12} m/V for sample B. It is clear from our measurements that waveguides with the quantum boxes show an *enhanced* electro-optic effect when compared to bulk GaAs, with a $4.5 \times$ increase between sample B and a value of 1.4×10^{-12} m/V for bulk GaAs.¹⁹

It should be cautioned that the exact form of the electro-optic coefficient or phase retardation in these lower-dimensional structures is not known exactly, and therefore

we call r_l an *effective* coefficient. Also, we assume that any quadratic effect is absent due to the large separation (~ 270 meV) between the excitation energy and the excitonic energy. More measurements are obviously necessary. However, the change on insertion of the boxes in the transmission region is very clear. Also clear is the increase in the built-in birefringence, which is the measured retardation at zero bias, as observed in Fig. 4. This is expected from the presence of the boxes.

In conclusion, we have shown a slight enhancement in the PL intensity for very small quantum boxes in the strained InGaAs/GaAs/AlGaAs system. Regrowth over the boxes and subsequent fabrication allowed us to demonstrate electro-optic waveguides with a greatly enhanced r_b , $4.5 \times$ that of bulk GaAs. We believe that this structure shows great potential for monolithic optoelectronic structures.

This work was supported by the Office of Naval Research under Contract N00014-90-J-1831 and the Army Research Office under Grant DAAL03-92-G0109.

¹G. Bryant, *Science and Engineering of One- and Zero-Dimensional Semiconductors*, edited by S. Beaumont and C. Torres (Plenum, New York, 1990), p. 243.

²G. Bryant, *Phys. Rev. B* **37**, 8763 (1988).

³S. Schmitt-Rink, D. Miller, and D. Chemla, *Phys. Rev. B* **35**, 8113 (1987).

⁴T. Takagahara, *Phys. Rev. B* **36**, 9293 (1987).

⁵Y. Miyamoto, Y. Miyake, M. Asada, and Y. Suematsu, *J. Quantum Electron.* **25**, 2001 (1989).

⁶Y. Arakawa, *22nd (1990 International) Conference on Solid State Devices and Materials*, Sendai (Business Center for Academic Societies, Tokyo, 1990), p. 745.

⁷A. Forchel, B. E. Maile, H. Leier, G. Mayer, and R. Germann, *Science and Engineering of One- and Zero-Dimensional Semiconductors*, edited by S. Beaumont and C. Torres (Plenum, New York, 1990), p. 277.

⁸C. Weisbuch, C. Sotomayor-Torres, and H. Benisty, *Nanostructures and Mesoscopic Systems* (Academic, San Diego, 1992), p. 471.

⁹P. Wang, C. Sotomayor-Torres, H. Benisty, C. Weisbuch, and S. Beaumont, *Appl. Phys. Lett.* **61**, 946 (1992).

¹⁰E. Colas, E. Kapon, S. Simhony, H. Cox, R. Bhat, K. Kash, and P. Lin, *Appl. Phys. Lett.* **55**, 867 (1989).

¹¹Y. Nagamune, M. Nishioka, S. Tsukamoto, and Y. Arakawa (to be published).

¹²T. Takahashi, Y. Arakawa, M. Nishioka, and T. Ikoma, *J. Cryst. Growth* (to be published).

¹³I. Tan, R. Mirin, V. Jayaraman, S. Shi, E. Hu, and J. Bowers, *Appl. Phys. Lett.* **61**, 300 (1992).

¹⁴H. Temkin, G. Dolan, M. Panish, and S. Chu, *Appl. Phys. Lett.* **50**, 413 (1987).

¹⁵T. Aizawa, K. Shimomura, S. Arai, and Y. Suematsu, *Photon. Technol. Lett.* **3**, 907 (1991).

¹⁶J. Patillon, C. Delalande, C. Jay, J. Andre, R. Gamonal, M. Iost, B. Soucaill, M. Voos, and G. Martin, *22nd (1990 International) Conference on Solid State Devices and Materials*, Sendai (Business Center for Academic Societies, Tokyo, 1990), p. 107.

¹⁷S. Pang, Y. Liu, and K. Sung, *J. Vac. Sci. Technol. B* **9**, 3530 (1991).

¹⁸D. Biswas, P. R. Berger, U. Das, J. E. Oh, and P. K. Bhattacharya, *J. Electron. Mater.* **18**, 137 (1989).

¹⁹A. Yariv and P. Yeh, *Optical Waves in Crystals* (Wiley, New York, 1984).